Archives of Biochemistry and Biophysics 766 (2025) 110331

Contents lists available at ScienceDirect

Archives of Biochemistry and Biophysics

journal homepage: www.elsevier.com/locate/yabbi

Eriodictyol 5-*O*-methyl ether inhibits prostate cancer progression through targeting STAT3 signaling and inducing apoptosis and paraptosis

Min Hee Yang [a,1], Ninh The Son [b,c,d,1], Jairo Kenupp Bastos [d], Nguyen Dinh Luyen [e], Nguyen Ngoc Linh [f], Kwang Seok Ahn [a,*]

[a] Department of Science in Korean Medicine, Kyung Hee University, 24 Kyungheedae-ro, Dongdaemun-gu, Seoul, 02447, Republic of Korea
[b] Institute of Chemistry, Vietnam Academy of Science and Technology (VAST), Hoang Quoc Viet, Caugiay, Hanoi, 10000, Viet Nam
[c] Department of Chemistry, Graduate University of Science and Technology, VAST, Hoang Quoc Viet, Caugiay, Hanoi, 10000, Viet Nam
[d] University of São Paulo (USP), School of Pharmaceutical Sciences of Ribeirão Preto, SP, Brazil
[e] Institute of Natural Products Chemistry, VAST, Hoang Quoc Viet, Caugiay, Hanoi, 10000, Viet Nam
[f] Faculty of Pharmacy, Thanh Do University, Kim Chung, Hoai Duc, Hanoi, 10000, Viet Nam

ARTICLE INFO

Keywords:
Eriodictyol 5-*O*-methyl ether
STAT3
Apoptosis
Autophagy
SHP-2

ABSTRACT

Prostate cancer ranks as one of the most prevalent cancers among men and is a major cause of cancer-related mortality globally This study aims to elucidate the molecular mechanisms underlying the anti-cancer effects of eriodictyol 5-*O*-methyl ether (ERIO) on prostate cancer cells, focusing on its impact on STAT3 signaling, apoptosis, and paraptosis. ERIO exhibited significant cytotoxicity against DU145, PC-3, and LNCaP cells. It suppressed constitutive and IL-6-induced STAT3 activation by inhibiting the phosphorylation of JAK1, JAK2, and Src kinases. ERIO upregulated SHP-2 expression, leading to the dephosphorylation of STAT3. ERIO induced apoptosis, evidenced by increased caspase-3 and PARP cleavage, and paraptosis, characterized by increased ROS production, decreased mitochondrial membrane potential, and ER stress. The antioxidant NAC reversed the effects of ERIO, highlighting the importance of oxidative stress in its anti-cancer activity. ERIO effectively inhibited prostate cancer cell growth by targeting STAT3 signaling and inducing both apoptosis and paraptosis. These findings suggest that ERIO has significant therapeutic potential for prostate cancer treatment and warrant further investigation in *in vivo* and clinical studies.

1. Introduction

Prostate cancer ranks as one of the most prevalent cancers among men and is a major cause of cancer-related mortality globally [1]. Advances in early diagnosis and treatment have been significant; however, prostate cancer continues to present substantial clinical challenges, especially when it progresses to castration-resistant prostate cancer (CRPC), which is known for its aggressiveness and resistance to conventional treatments [2,3]. Despite the efficacy of current treatments like surgery, radiation, hormone therapy, and chemotherapy, resistance remains a significant hurdle [4,5].

Cell death mechanisms are crucial in controlling cancer progression and treatment response. Apoptosis, or programmed cell death, involves a series of cellular events leading to cell shrinkage, chromatin condensation, DNA fragmentation, and eventual cell death [6,7]. It is a vital process for eliminating damaged or unnecessary cells and maintaining tissue homeostasis. The intrinsic apoptotic pathway is triggered by internal signals such as DNA damage and oxidative stress, leading to mitochondrial outer membrane permeabilization and the release of cytochrome *c*, which activates caspases to execute cell death [8]. On the other hand, the extrinsic pathway is initiated by external signals such as ligand binding to death receptors on the cell surface, leading to caspase activation [7,9].

Paraptosis, in contrast, is a type of programmed cell death distinct from apoptosis. It is characterized by cytoplasmic vacuolation and mitochondrial swelling, which sets it apart from apoptosis in both

* Corresponding author. Department of Science in Korean Medicine, College of Korean Medicine, Kyung Hee University, 24 Kyungheedae-ro, Dongdaemun-gu, Seoul, 02447, Republic of Korea.
E-mail addresses: didmini@naver.com (M.H. Yang), yamantson@gmail.com (N.T. Son), jkbastos@fcfrp.usp.br (J.K. Bastos), dinhluyen1085@gmail.com (N.D. Luyen), nnlinh@thanhdouni.edu.vn (N.N. Linh), ksahn@khu.ac.kr (K.S. Ahn).
[1] These authors contributed equally to this work and therefore equal first authors.

https://doi.org/10.1016/j.abb.2025.110331
Received 26 August 2024; Received in revised form 20 January 2025; Accepted 6 February 2025
Available online 7 February 2025
0003-9861/© 2025 Published by Elsevier Inc.

morphology and biochemistry [10]. Unlike apoptosis, paraptosis does not involve caspase activation or DNA fragmentation. Instead, it is associated with the dilation of the endoplasmic reticulum and mitochondrial swelling, leading to cell death through a mechanism that remains less well understood [10,11]. The discovery of paraptosis has broadened the understanding of cell death mechanisms and highlighted the complexity of cellular responses to stress and damage. The interplay between apoptosis and paraptosis is complex, and understanding how these pathways can be manipulated offers promising avenues for cancer treatment. By inducing both forms of cell death, therapies can potentially eliminate cancer cells more effectively, reduce the likelihood of resistance, and improve patient outcomes. The exploration of drugs that can trigger both apoptosis and paraptosis, therefore, represents a significant area of interest in cancer research [12–15].

Signal Transducer and Activator of Transcription 3 (STAT3) is a crucial molecule in many cellular processes, such as cell growth, survival, and immune response [16]. Abnormal activation of STAT3 has been linked to the development and progression of various cancers, including prostate cancer [16–19]. STAT3 aids tumor growth and survival by regulating genes involved in cell proliferation, inhibition of apoptosis, and immune system evasion [20]. Importantly, STAT3 activation can block apoptosis by increasing the expression of anti-apoptotic genes like Bcl-2 and Bcl-xL, thus aiding cancer cell survival [20,21]. Additionally, STAT3 has been implicated in the regulation of paraptosis, though the precise mechanisms are still under study [22,23]. By affecting these pathways, STAT3 plays a critical role in cancer cell resistance to treatment. Therefore, targeting the STAT3 pathway is a promising approach for cancer therapy, aiming to induce both apoptosis and paraptosis to enhance treatment outcomes. SHP-2 (Src Homology 2 domain-containing Phosphatase-2) is a protein tyrosine phosphatase that plays a critical role in the regulation of the STAT3 signaling pathway. SHP-2 can dephosphorylate STAT3, thereby negatively regulating its activity and affecting downstream signaling events [24,25]. Dysregulation of SHP-2 has been associated with enhanced STAT3 activity, contributing to cancer cell survival and proliferation [26]. Therefore, targeting SHP-2 along with STAT3 could offer a comprehensive strategy to induce both apoptosis and paraptosis, thereby enhancing the therapeutic efficacy against prostate cancer [27].

Nature is a rich source of bioactive secondary metabolites, substances produced by bacteria, fungi, plants, and other organisms [22]. These metabolites often possess beneficial properties such as anticancer, antibacterial, antioxidant, and anti-inflammatory activities. Examples include plant flavonoids, fungal polyketides, and bacterial antibiotics. These organic compounds remain a critical source of novel bioactive molecules with potential therapeutic applications and have inspired the development of numerous drugs. In this study, we isolated and purified the flavanone eriodictyol 5-*O*-methyl ether (ERIO) from Brazilian *Mimosa tenuiflora* green propolis, collected by Africanized honeybees (*Apis mellifera* L.), and evaluated its anticancer effects, particularly its ability to induce apoptosis and paraptosis by targeting the STAT3 signaling pathway in prostate cancer cells. This research aims to uncover the molecular mechanisms by which eriodictyol 5-O-methyl operates, providing a fundamental basis for the development of new therapeutic approaches targeting these cell death pathways.

2. Material and methods

2.1. General experimental procedure

NMR spectral data (400 MHz for ^{1}H and 100 MHz for ^{13}C NMR) were obtained from a Bruker AVANCE in methanol-d_4. Silica gel (40–63 μm; Merk, Sigma-Aldrich) and preparative HPLC-DAD (High-Performance Liquid Chromatography, United States) were used to perform column chromatography. Thin Layer Chromatography (TLC) was carried out using silica gel 60 F_{254} (Merck, Germany). H_2SO_4 10 % in EtOH was used for the TLC observation.

2.2. Plant material

M. tenuiflora green propolis was produced by Africanized honeybees (*Apis mellifera* L.) in Remanso, Bahia, Brazil and collected in June 2021. The plant was taxonomically identified and the voucher specimen (SPFR: 15118) was stored at the Herbarium of the Department of Biology, University of São Paulo, Ribeirão Preto, SP, Brazil.

2.3. Reagents

Antibodies, (STAT3, SHP-2, PARP, Src, Bcl-2, IAP-1, Alix, and β-actin) was purchased from Santa Cruz Biotechnology (Santa Cruz, CA, USA). Other Antibodies (p-STAT3, p-JAK1, p-JAK2, JAK1, JAK2, p-Src, Cyclin D1, ATF4, and CHOP) were procured from Cell signaling Technology (Beverly, MA, USA).

2.4. Cell lines and culture conditions

Human prostate cancer DU145, PC-3, LNCaP and prostate normal RWPE-1 cells were obtained from American Type Culture Collection (Manassas, VA, USA). DU145, PC-3, LNCaP, and RWPE-1 cells were cultured in RPMI6140 medium and maintained at 37 °C under 5 % CO_2 conditions. The medium supplemented with 10 % fetal bovine serum (FBS) and 1 % antibiotic solution.

2.5. MTT assay

DU145, PC-3, LNCaP, and RWPE-1 cells were treated with (0, 10, 30, 50, 100 μM) of ERIO for 24 h and MTT assay was performed as described earlier [28].

2.6. Western blot analysis

Whole cell lysates were prepared and Western blot analysis for various antibodies was carried out as elaborated earlier [29]. Equal amount of proteins were resolved in sodium dodecyl sulfate-polyacrylamide gel electrophoresis (SDS-PAGE) gel and transferred into the nitrocellulose membrane. Membranes were incubated with primary antibodies (1:3000) in TBST overnight, then incubated with secondary antibody (1:5000) for 1 h. Detection was carried out using enhanced chemiluminescence (ECL, EZ-Western Lumi Femto, DOGEN).

2.7. Immunocytochemistry

Cells were treated with ERIO (100 μM) for 6 h and expression of p-STAT3 and STAT3 was analyzed through immunocytochemistry as reported previously [28]. The fluorescence signal was detected by Olympus FluoView FV1000 confocal micro-scope (Tokyo, Japan).

2.8. Cell cycle analysis

The effect of ERIO on cell cycle progression was examined by cell cycle analysis as described before [28]. After treatment, cells were fixed with EtOH (100 %) overnight at 4 °C. The next day, cells were resuspended with RNase A for 1 h. Then, cells were stained with PI and analyzed by BD AccuriTM C6 Plus Flow Cytometer (BD Biosciences, Becton-Dickinson).

2.9. TUNEL assay

Cells were treated with ERIO (100 μM) for 24 h and TUNEL assay was performed as reported earlier [22]. The cells were stained with TUNEL enzyme and label for 1 h, then cells were analyzed by BD AccuriTM C6 Plus Flow Cytometer (BD Biosciences, Becton-Dickinson).

2.10. Live and dead assay

DU145 and PC-3 cells were treated with ERIO (100 μM) for 24 h and Live and dead cells was carried out as described previously [22]. The cells were stained with 1 μL/mL of Calcein AM and 2 μL/mL of Ethd-1 at 37 °C for 30 min (Invitrogen, Carlsbad, CA, USA). The cells were attached on slide glass by cytospin. The fluorescence signals were detected by Olympus FluoView FV1000 confocal micro-scope (Tokyo, Japan).

2.11. Reactive Oxygen Species (ROS) assay

The cells were treated with ERIO (100 μM) or NAC (3 mM). Then cells incubated with 2′,7′-dichlorofluorescin diacetate (H_2DCF-DA) and detected by BD AccuriTM C6 Plus Flow Cytometer (BD Biosciences, Becton-Dickinson).

2.12. Mitochondrial membrane potential assay

The cells were treated with ERIO (100 μM) for 24 h. Then, they were stained with TMRE 50 nM for 30 min and detected by BD AccuriTM C6 Plus Flow Cytometer (BD Biosciences, Becton-Dickinson).

2.13. ER stress assay

DU145 and PC-3 cells were treated with ERIO (100 μM) for 24 h and cells were stained by ER-tracker red (1 μM) and DAPI (10 μg/ml). Then, cells were detected by Olympus FluoView FV1000 confocal micro-scope (Tokyo, Japan).

2.14. Statistical analysis

The results were expressed as means ± standard deviation (SD), and an analysis of variance (ANOVA) with Bonferroni's test was used for the statistical analysis of multiple comparisons of data. p-value of 0.05 or less was considered as significant.

3. Results

3.1. Extraction and isolation of ERIO

The propolis powders (1.0 kg) were ground in a blender, and immersed in 3 L of EtOH–H_2O (7:3, v/v, 3 times) at 25 °C for 24 h, and then filtered. The obtained extract was vacuum-evaporated, and lyophilized until dry. This residue (25.5 g) was chromatographed on silica gel column chromatography (*n*-hexane-acetone, 3:1, v/v, and CH_2Cl_2-EtOAc, 9:1, v/v), and HPLC-DAD (MeOH–H_2O, 6:4, v/v) to yield 60.1 mg of eriodictyol 5-*O*-methyl ether (Fig. 1 and Supplementary Material).

3.2. ERIO exhibited cytotoxic activity against DU145, PC-3, and LNCaP cells

The chemical structure of ERIO is depicted in Fig. 1A. The cytotoxic activity of ERIO against prostate cancer cells and prostate normal RWPE-1 cells were examined by MTT assay. As shown in Fig. 1B, ERIO significantly suppressed the viability of DU145, PC-3, and LNCaP cells. However, it was only slightly affected in the RWPE-1 cells.

3.3. ERIO suppressed constitutive STAT3 activation in prostate cancer cells

We first examined the impact of ERIO on STAT3 activation. DU145 and PC-3 cells were treated with various concentrations and time intervals of ERIO and western blotting was carried out. As shown in Fig. 1C and D, constitutive STAT3 activation was suppressed upon ERIO treatment. Moreover, as shown in Fig. 1E, ERIO exposure inhibited the nuclear translocation of STAT3 protein therefore preventing the gene transcription.

3.4. ERIO decreased activation of STAT3 upstream kinases

Next, we determined whether ERIO could alter the levels of kinases involved the activation of STAT3. Phosphorylation of STAT3 can be driven through the stimulation of Janus activated kinases (JAK) and Src families of proteins [30]. As shown in Fig. 1F and G, ERIO inhibited the phosphorylation of JAK1, JAK2, and Src kinases in prostate cancer DU145 and PC-3 cells.

3.5. ERIO down-regulated inducible STAT3 activation

LNCaP cells were treated with 100 μM of ERIO for (0, 2, 4, 6 h) and stimulated with IL-6 (10 ng/ml) for 15 min. ERIO suppressed IL-6-induced STAT3 phosphorylation (Fig. 2A). ERIO also altered JAK1/2 and Src activation in LNCaP cells (Fig. 2B).

3.6. ERIO induced SHP-2 expression

We investigated the mechanism of ERIO stimulated inhibition of STAT3 activation. Protein tyrosine phosphatases (PTPs) have been reported as STAT activation regulators. As shown in Fig. 2C, sodium pervanadate reversed the mitigation of STAT3 phosphorylation, highlighting that this activity of ERIO can be regulated by a tyrosine phosphatase. We noted that ERIO treatment increased SHP-2 expression (Fig. 2D). To confirm whether ERIO attenuate STAT3 activation through promoting SHP-2 expression, we performed SHP-2 knockdown experiment. We observed that ERIO-induced SHP-2 expression was altered in the SHP-2 siRNA transfected cells. However, deletion of SHP-2 altered ERIO-induced p-STAT3 down-regulation (Fig. 2E). These results suggested that ERIO modulated STAT3 activation through up-regulating the expression of SHP-2. Additionally, we conducted STAT3 siRNA experiments to determine whether STAT3 downregulation was related to ERIO-induced apoptosis and paraptosis. As shown in Fig. 2F, ERIO-induced apoptosis and paraptosis were promoted upon transfection with STAT3 siRNA as compared with the scrambled siRNA. These findings suggest that the induction of ERIO-induced cell death is mediated at least in part through the mitigation of the STAT3 signaling pathway.

3.7. ERIO promoted apoptosis

We investigated the impact of ERIO on apoptotic cell death in DU45 and PC-3 cells. As shown in Fig. 3A, ERIO induced cell population in subG1 phase in DU145 cells. ERIO also enhanced cell population in subG1 and G0/G1 phase. We observed that ERIO induced apoptosis and significantly attenuated viability of prostate cancer cells (Fig. 3B and C). Moreover, we found that ERIO promoted apoptosis by increasing caspase-3 and PARP cleavage (Fig. 3D). ERIO also down-regulated the apoptotic markers (Fig. 3E). Additionally, as shown in Fig. 3E, knockdown of SHP-2 also mitigated induction of PARP cleavage by ERIO. This result suggested that SHP-2 may play crucial role in regulating anticancer activities of ERIO.

3.8. ERIO induced paraptosis

We examined whether ERIO induced changes in ROS production and mitochondrial membrane potential. As shown in Fig. 4A and B, ERIO treatment increased ROS production and decreased mitochondrial membrane potential. Prostate cancer cells were treated with ERIO and stained with ER-tracker red to examined the expression of the key transcription factors involved in the ER stress pathway. As shown in Fig. 4C, ER staining indicated that vacuolization was obtained primarily

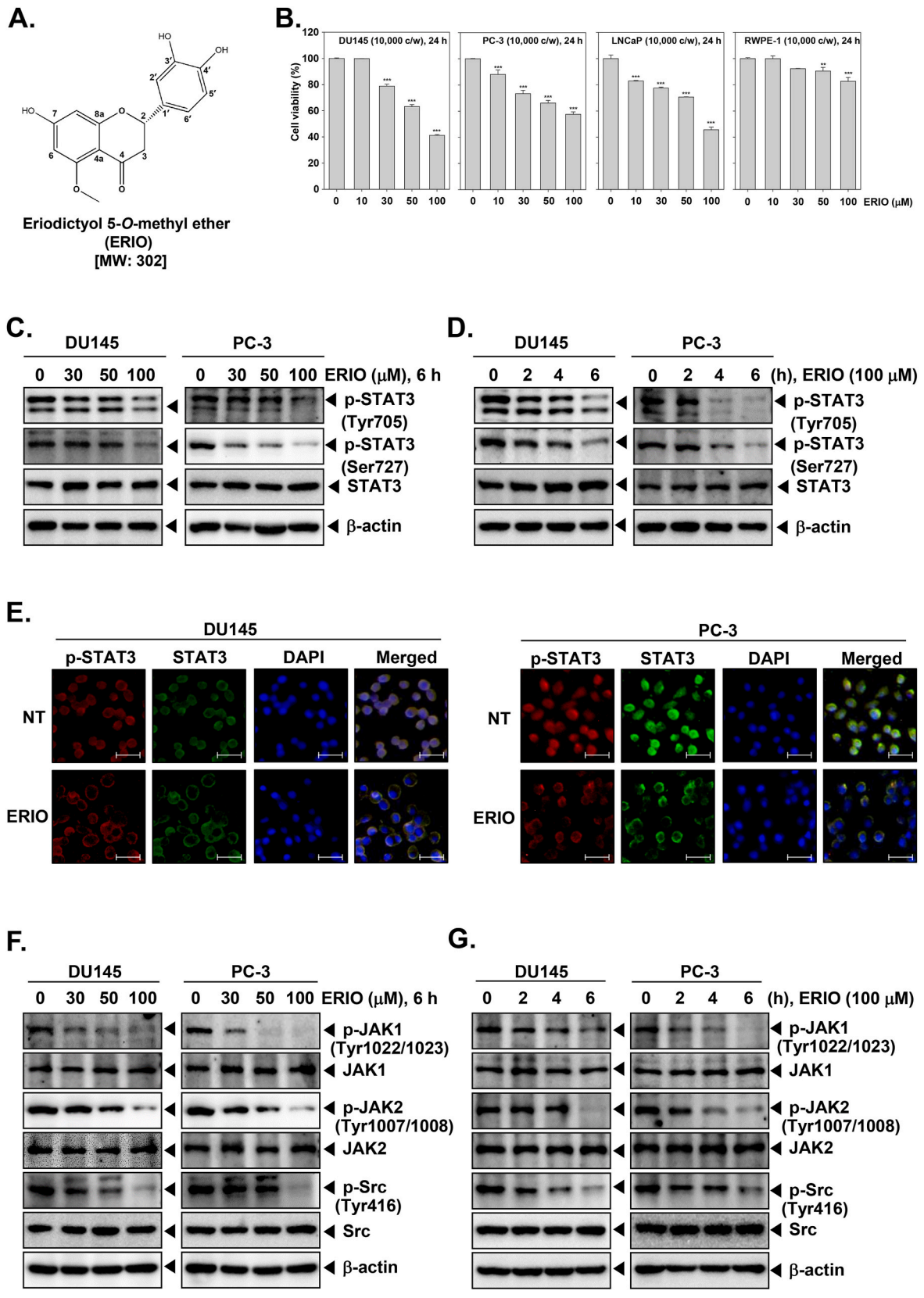

Fig. 1. ERIO suppresses constitutive STAT3 activation in DU145 and PC-3 cells. (A) The chemical structure of ERIO. **(B)** DU145, PC-3, LNCaP, and RWPE-1 cells were treated with ERIO (0, 10, 30, 50, 100 μM) for 24 h and MTT assay was carried out. Data represents mean ± SD. ***$p < 0.001$ vs. non-treated (NT) cells. **(C and D)** DU145 and PC-3 cells were treated with various concentrations and time intervals. Western blot analysis for p-STAT3(Tyr705), p-STAT3(Ser727), STAT3, and β-actin was performed. **(E)** Expression of p-STAT3 and STAT3 in DU145 and PC-3 cells was elaborated with immunocytochemistry **(F and G)** The cells were treated with ERIO and Western blotting for p-JAK1(Tyr1022/1023), JAK1, p-JAK2(Tyr1007/1008), JAK2, p-Src(Tyr416), Src, and β-actin was performed. The results shown are representative of the three independent experiments.

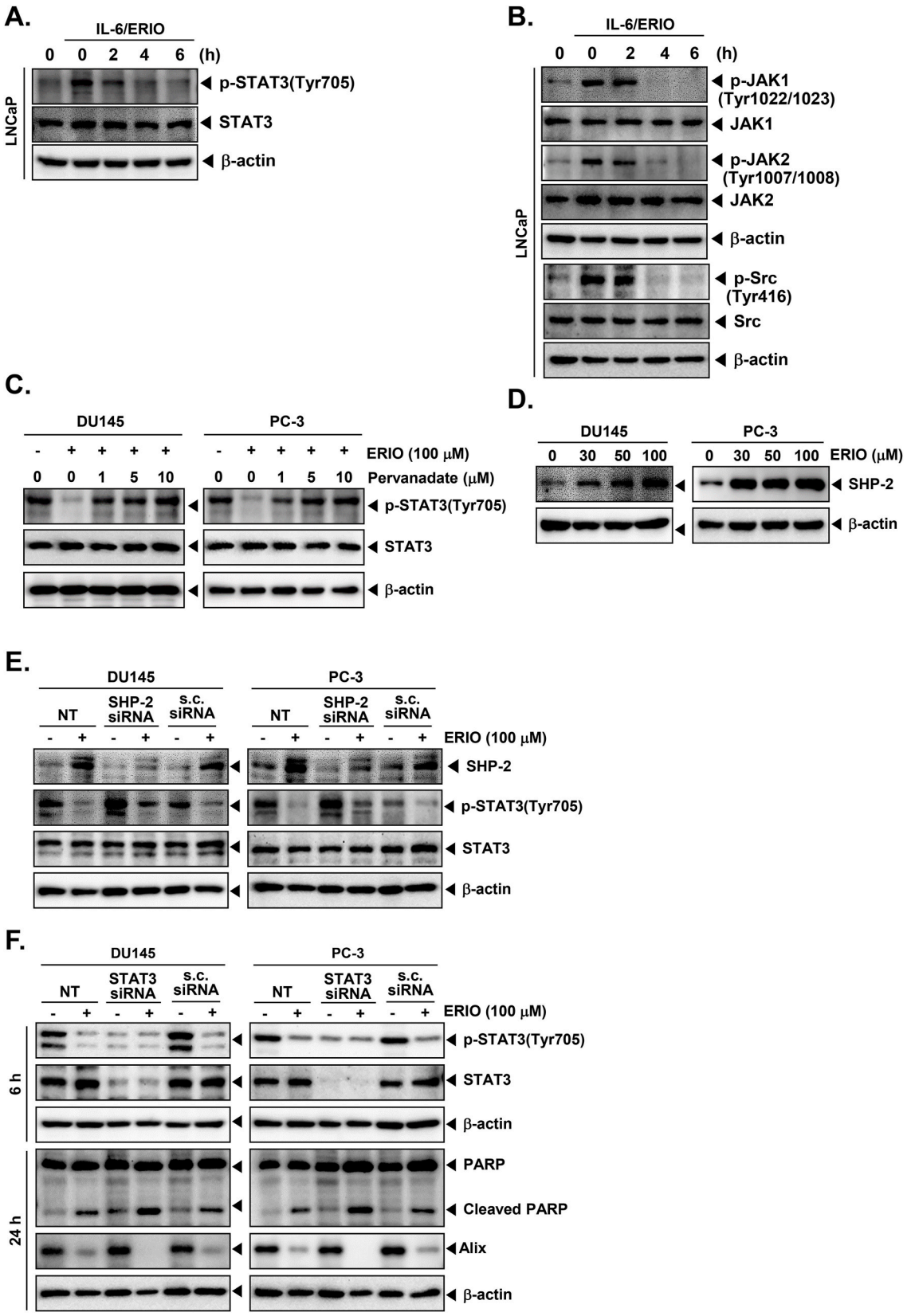

Fig. 2. ERIO suppresses inducible STAT3 phosphorylation and increases the level of SHP-2. **(A–B)** LNCaP cells were treated with ERIO (100 μM) and stimulated with IL-6 (10 ng/ml) and Western blotting was executed. **(C)** DU145 and PC-3 cells were treated with ERIO and pervanadate and immunoblotting for p-STAT3 and STAT3 was performed. **(D)** The cells were treated with ERIO for 6 h and Western blotting for SHP-2 was carried out. **(E)** cells were transfected with SHP-2 siRNA or scrambled siRNA (100 nM). After 24 h, the cells were treated with ERIO (100 μM) for 6 h and Western blot analysis was performed. **(F)** DU145 and PC-3 cells were transfected with STAT3 siRNA or scrambled siRNA (100 nM) for 24 h. Then, the cells were treated with ERIO (100 μM) for 6 or 24 h. Western blotting for various antibodies was carried out. The results shown are representative of the three independent experiments.

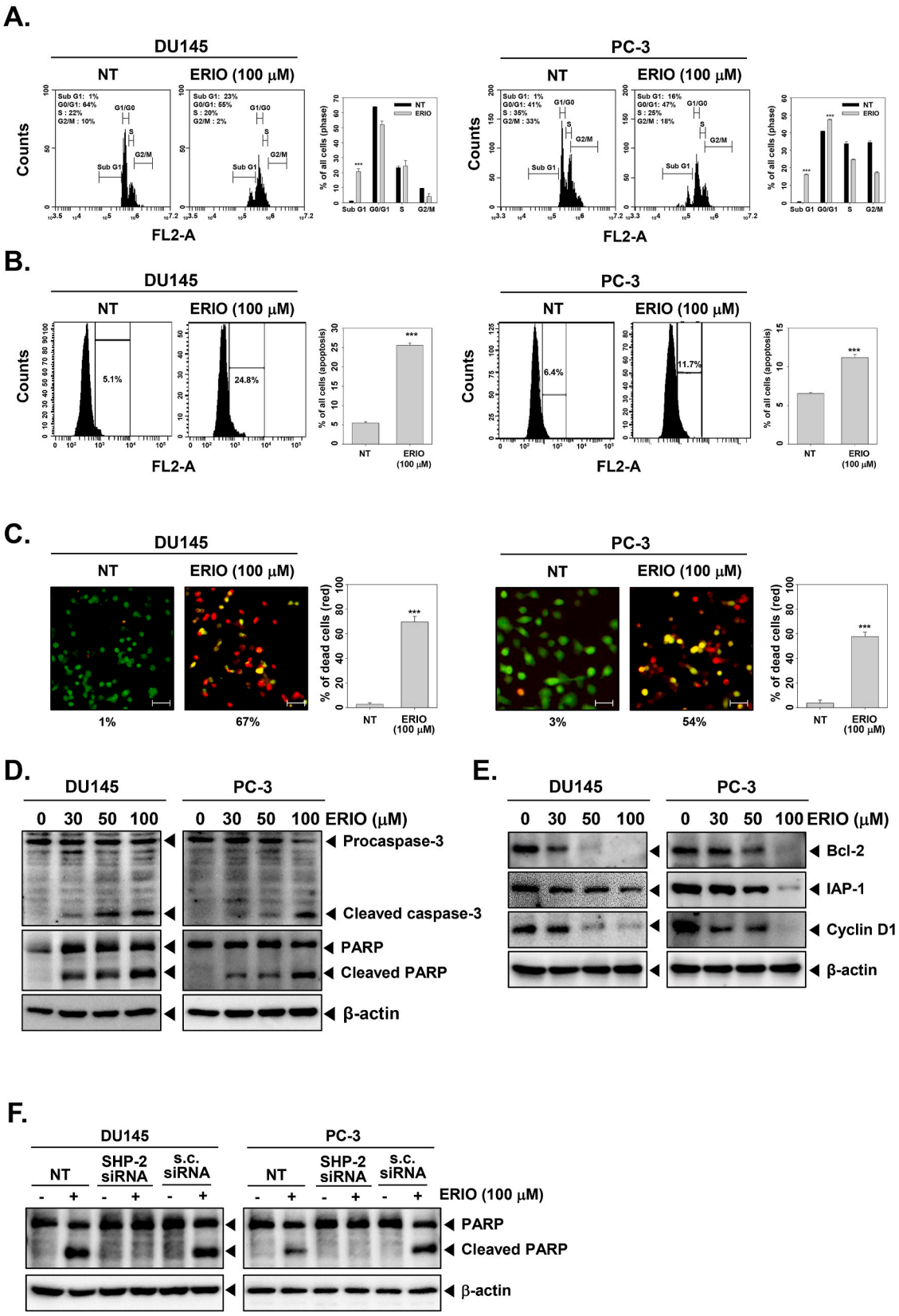

Fig. 3. ERIO induces apoptosis in prostate cancer cells. (A and B) DU145 and PC-3 cells were treated with ERIO (100 μM) for 24 h and cell cycle analysis and TUNEL assay was carried out. Data represents mean ± SD. ***$p < 0.001$ vs. non-treated (NT) cells. **(C)** Cells were treated with ERIO and live and dead assay was performed. **(D and E)** The cells were treated with ERIO (0,30, 50,100 μM) for 24 h and wester blotting for various antibodies was done. Data represents mean ± SD. ***$p < 0.001$ vs. non-treated (NT) cells. **(F)** DU145 and PC-3 cells were transfected with SHP-2 siRNA or scrambled siRNA (100 nM). After 24 h, cells were treated with ERIO (100 μM) for 24 h and immunoblotting for PARP was carried out. The results shown are representative of the three independent experiments.

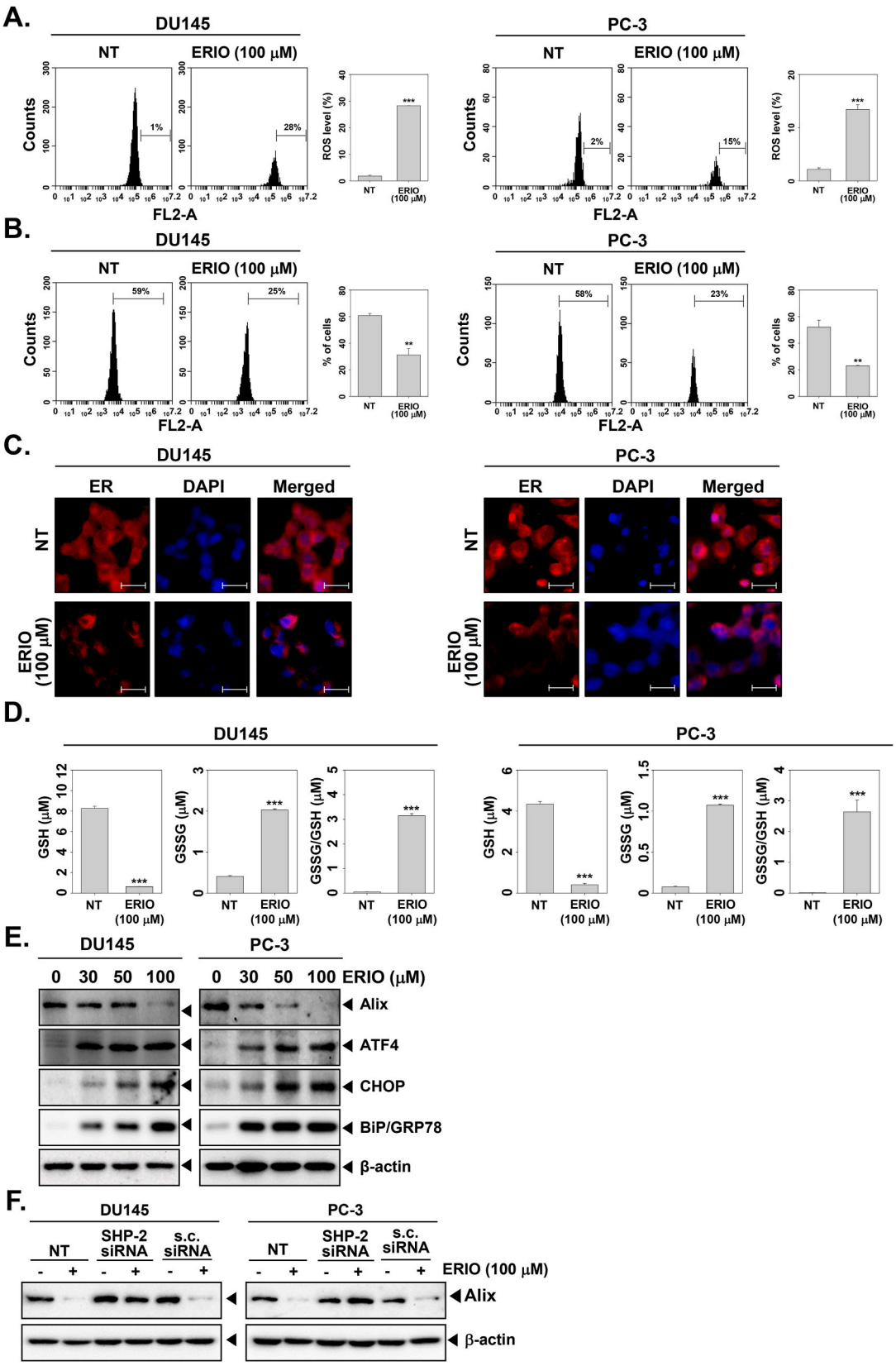

Fig. 4. ERIO induces paraptosis in prostate cancer cells. (A and B) DU145 and PC-3 cells were treated with ERIO (100 μM) for 24 h and ROS assay and mitochondrial membrane potential assay was carried out. Data represents mean ± SD. $^{**}p < 0.01$ vs. non-treated (NT) cells. $^{***}p < 0.001$ vs. non-treated (NT) cells. **(C)** Cells were treated with ERIO and ER stress assay was performed. **(D)** The cells were treated as described above in panel A, GSH/GSSG assay was executed. **(E)** The cells were treated with ERIO (0, 30, 50,100 μM) for 24 h and wester blotting for Alix, ATF4, CHOP, BiP/GRP78, and β-actin was done. **(F)** DU145 and PC-3 cells were transfected with SHP-2 siRNA or scrambled siRNA (100 nM). After 24 h, cells were treated with ERIO (100 μM) for 24 h and immunoblotting for Alix was carried out.

from the ER. As shown in Fig. 4D, the depletion of GSH was observed, and the GSSG and GSSG/GSH ratio was increased, indicating oxidative stress. We found that ERIO induced paraptosis by suppressing Alix, and increasing ATF4, CHOP, and BiP/GRP78 expressions (Fig. 4E). Additionally, as shown in Fig. 4F, knockdown of SHP-2 altered attenuation of Alix by ERIO. This result suggested that SHP-2 may play key role in regulating anti-cancer activities of ERIO.

3.9. NAC revered ERIO induced apoptosis and paraptosis

To further establish the role of N-acetylcysteine (NAC) in ERIO-treated cells on anti-cancer activities of ERIO, we conducted experiments using ERIO and antioxidant NAC. As demonstrated in Fig. 5A, the ERIO treatment significantly increased the ROS levels and NAC prevents ROS production. As shown in Fig. 5B, NAC mitigated ERIO-induced SHP-2 expression and p-STAT3 down-regulation. Also, ERIO treatment induced the PARP cleavage and reduced the expression of Alix, but NAC prevented the changes (Fig. 5C). These results suggested that NAC revers ERIO induced apoptosis and paraptosis. Additionally, to determine the timing of ERIO-induced apoptosis and paraptosis, we monitored changes in PARP cleavage and Alix after administering ERIO in a time-dependent manner. As illustrated in Fig. 5D, in both DU145 and PC-3 cells, PARP cleavage occurred prior to the reduction in Alix. Moreover, cell death occurred sooner in DU145 cells compared to PC-3 cells, and in DU145 cells, no band was visible after 36 h due to cell death from cytotoxicity. We also used cycloheximide (CHX), a paraptosis inhibitor [31,32], to confirm ERIO-induced paraptosis. As illustrated in Fig. 5E, the simultaneous administration of ERIO and CHX diminished the suppression of Alix expression caused by ERIO alone. Moreover, the combination of ERIO and CHX resulted in a smaller reduction in cell viability compared to the treatment with only ERIO (100 μM) as shown in Fig. 5F. These findings suggest that CHX can mitigate the effects of ERIO-induced paraptosis, specifically by stabilizing Alix expression, indicating a potential protective role against cytotoxicity induced by ERIO. Moreover, the reduced decrease in cell viability when ERIO was combined with CHX highlights the potential for CHX to modulate the therapeutic effects of ERIO, which could be important for optimizing treatment strategies (see Fig. 6).

4. Discussions

The findings of this study reveal that ERIO, a novel compound can significantly inhibit prostate cancer cell growth by inducing apoptosis and paraptosis. It achieved these effects through the dual mechanisms of inhibiting the STAT3 signaling pathway and upregulating SHP-2. The comprehensive methodology employed in this research offers crucial insights into the underlying mechanisms by which ERIO operates and underscores its potential therapeutic benefits for treating prostate cancer. This dual mechanism of action not only can disrupt cancer cell survival pathways but also can activate cellular processes that promote cancer cell death, thereby making ERIO a promising candidate for future prostate cancer therapies.

STAT3 is known to play a crucial role in the proliferation and survival of cancer cells, and its persistent activation is often associated with poor prognosis in various cancers, including prostate cancer [22,33]. By inhibiting STAT3 activation and preventing its nuclear translocation, ERIO effectively disrupts the downstream gene transcription that promotes tumor growth and survival. This suppression of STAT3 is mediated through the inhibition of its upstream kinases, JAK1, JAK2, and Src [24,34,35]. Moreover, ERIO was found to down-regulate inducible STAT3 activation in response to IL-6 stimulation. The IL-6/STAT3 axis is a well-established pathway in cancer biology, contributing to tumor progression [36]. Our data indicate that ERIO can inhibit this pathway, thus enhancing its therapeutic potential by targeting both constitutive and inducible STAT3 activation mechanisms. SHP-2 can dephosphorylate STAT3, thereby negatively regulating its activity and affecting downstream signaling events [24,25]. Dysregulation of SHP-2 has been associated with enhanced STAT3 activity, contributing to cancer cell survival and proliferation [26]. We found that ERIO was able to upregulate SHP-2 expression. The knockdown experiments further validated the critical role of SHP-2 in mechanism of action of ERIO, as reducing SHP-2 levels negated ERIO's effects on STAT3 phosphorylation, and the induction of apoptosis and paraptosis.

Since apoptosis is one of the important anti-cancer processes, we investigated the ERIO -induced apoptotic cell death. We found that ERIO was able to promote apoptosis in prostate cancer cells by increasing the subG1phase accumulation, enhancing caspase-3 and PARP cleavage, and down-regulating apoptotic markers. Interestingly, we observed that ERIO induced not only apoptosis but also paraptosis. Recent research has shown that paraptosis can be induced by specific stimuli, such as certain drugs and natural compounds, suggesting it could be a viable target for cancer therapy [37]. For instance, compounds like celastrol and withaferin A have been shown to induce paraptosis in cancer cells, providing a potential alternative to overcome resistance to apoptosis-inducing therapies [38,39]. Targeting multiple cell death pathways, including both apoptosis and paraptosis, may enhance the efficacy of anticancer therapies and help to circumvent resistance mechanisms that allow cancer cells to survive conventional treatments [15,22,40].

In our study, we identified key paraptosis-related factors, including Alix, ATF4, and CHOP, which were modulated upon ERIO treatment. Alix, a critical regulator of paraptosis, sees decreased expression linked to key characteristics of this non-apoptotic cell death pathway, including ER swelling and mitochondrial dysfunction [41]. To further elucidate the temporal dynamics of ERIO-induced cell death, we analyzed the time-dependent changes in PARP cleavage and Alix expression. Interestingly, Notably, the cleavage of PARP, a sign of apoptosis, occurred before the reduction in Alix, which signals paraptosis. This suggests that apoptosis may initially prepare the cells for subsequent paraptotic events. Additionally, we observed a significant increase in BiP/GRP78 expression after ERIO treatment, underscoring the importance of ER stress in triggering paraptosis. BiP/GRP78 is essential in managing cellular stress and facilitating non-apoptotic death pathways like paraptosis [42,43]. The concurrent upregulation of ATF4 and CHOP suggests that ERIO-induced ER stress triggers an adaptive UPR response, which eventually shifts towards cell death signaling under prolonged stress conditions.

Additionally, the use of the antioxidant N-acetylcysteine (NAC) revealed the importance of ROS in the mechanism of action of ERIO. NAC reversed the ERIO-induced ROS production, SHP-2 expression, STAT3 down-regulation, and PARP cleavage, indicating that oxidative stress plays a pivotal role in ERIO-induced apoptosis and paraptosis. Taken together, these results highlight the dual action of ERIO in inducing apoptosis and paraptosis, potentially through interconnected pathways involving ROS generation, ER stress, and modulation of critical regulatory proteins such as BiP/GRP78, ATF4, and CHOP. This comprehensive targeting of cell death pathways offers a promising therapeutic approach for treating prostate cancer, especially in scenarios where traditional therapies that primarily induce apoptosis are ineffective. By simultaneously activating both apoptotic and paraptotic pathways, ERIO may circumvent resistance mechanisms in cancer cells, potentially leading to more effective treatment outcomes. This strategy could broaden the spectrum of therapeutic options available for prostate cancer, emphasizing the importance of targeting multiple cell death mechanisms in overcoming drug resistance.

In conclusion, this study provides compelling evidence that ERIO exerts potent anticancer effects in prostate cancer cells by inducing apoptosis and paraptosis through the inhibition of the STAT3 pathway and the upregulation of SHP-2. The dual targeting of STAT3 and SHP-2, along with the induction of oxidative stress, represents a novel and effective strategy for overcoming resistance in prostate cancer treatment. Future studies should explore the clinical applicability of ERIO,

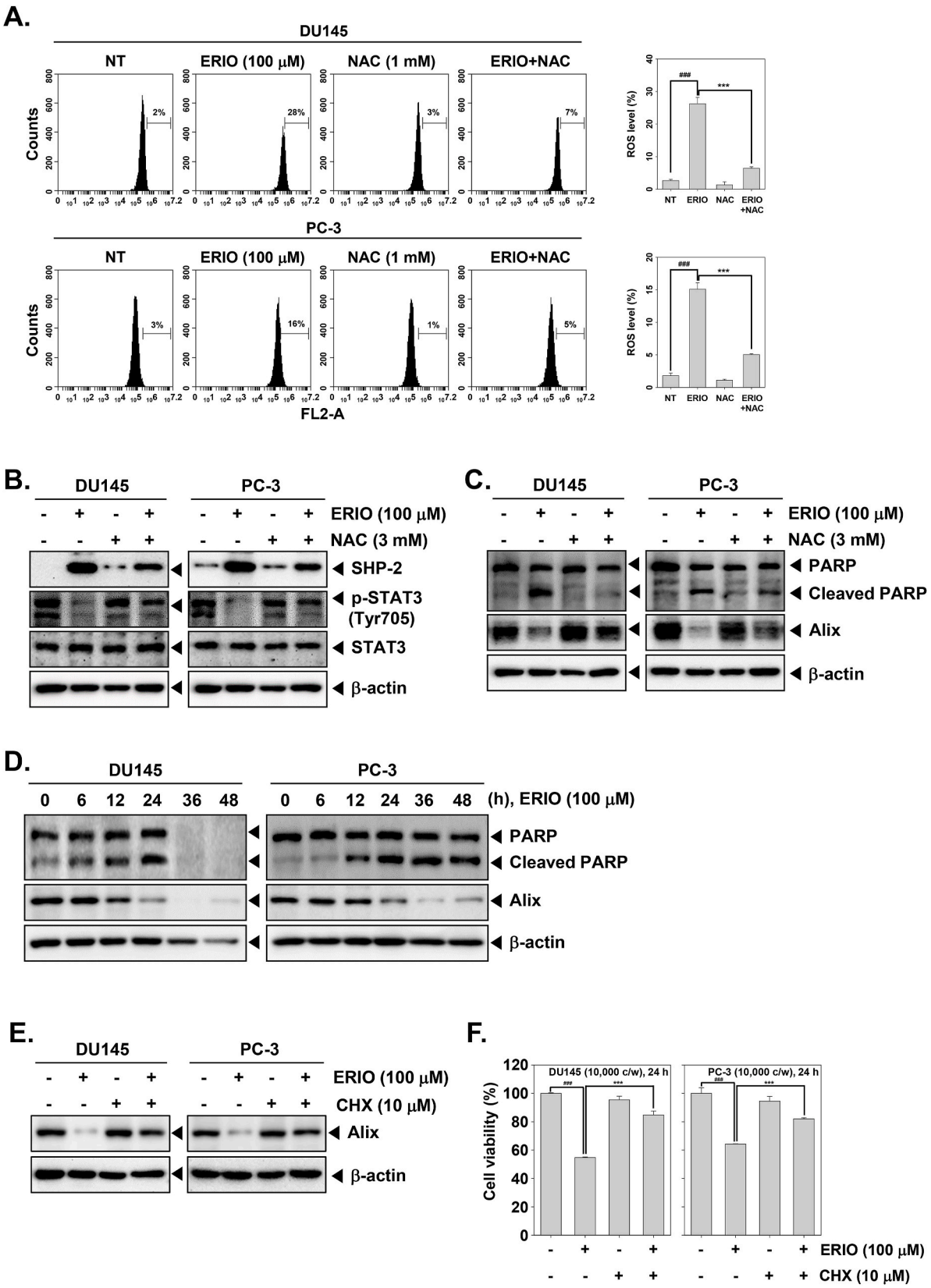

Fig. 5. ERIO increases ROS production. (A) DU145 and PC-3 cells were treated with ERIO (100 μM) or NAC (1 mM) for 24 h and ROS assay was performed. $^{###}p < 0.001$ vs. non-treated (NT) cells. $^{***}p < 0.001$ vs. ERIO-treated cells. **(B and C)** The cells were treated as described above in panel A, Western blotting for various proteins was elaborated. **(D)** The cells were treated with ERIO (100 μM) for (0, 6, 12, 24, 36, 48 h) and immunoblotting for PARP and Alix was carried out. **(E)** The cells were treated with ERIO (100 μM) or CHX (10 μM) for 24 h. Then, expressions of PARP and Alix were evaluated by Western blot analysis was performed. **(F)** The cells were treated as described above in panel E and MTT assay was carried out. Data represents mean ± SD. $^{###}p < 0.001$ vs. non-treated (NT) cells. $^{***}p < 0.001$ vs. ERIO (100 μM) treated cells. The results shown are representative of the three independent experiments.

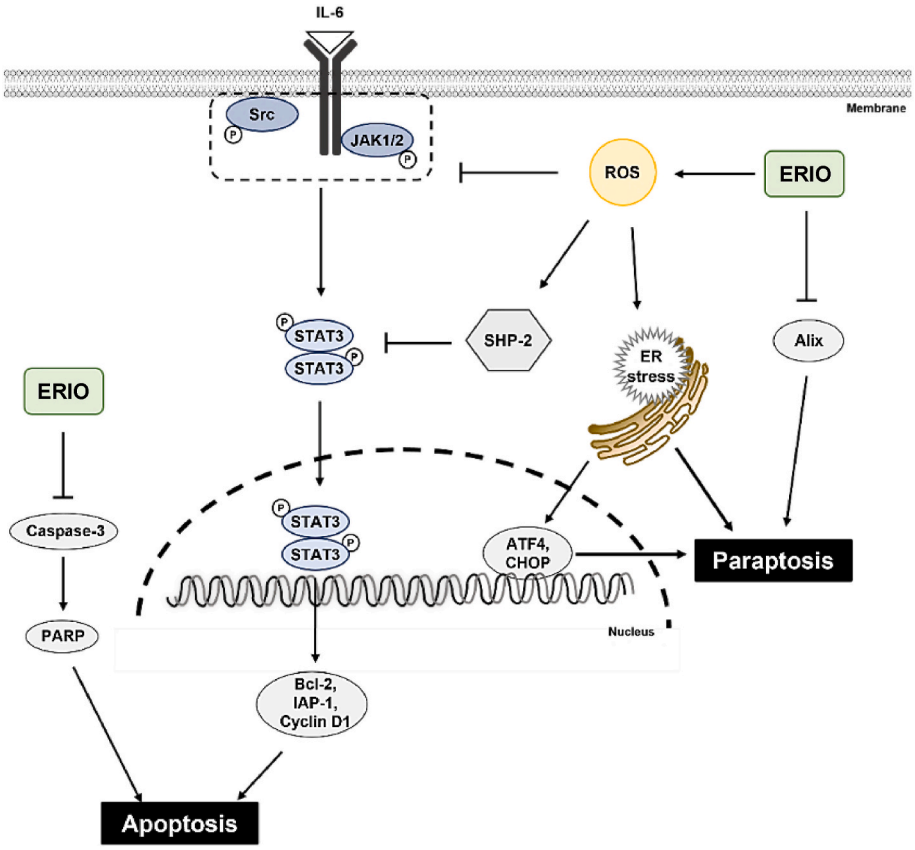

Fig. 6. A schematic diagram showing the effect of ERIO.

including its efficacy *in vivo*. Additionally, understanding the precise molecular mechanisms and potential side effects will be crucial for the development of ERIO as a therapeutic agent.

CRediT authorship contribution statement

Min Hee Yang: Writing – original draft, Investigation, Formal analysis, Conceptualization. **Ninh The Son:** Resources, Investigation, Formal analysis. **Jairo Kenupp Bastos:** Resources, Methodology. **Nguyen Dinh Luyen:** Validation, Formal analysis. **Nguyen Ngoc Linh:** Methodology, Data curation. **Kwang Seok Ahn:** Writing – review & editing, Validation, Supervision, Project administration, Methodology, Conceptualization.

Declaration of competing interest

The authors have no conflicts of interest to declare.

Acknowledgements

This work was supported by a National Research Foundation of Korea (NRF) grant funded by the Korean government (MSIP) (NRF-2021R1I1A2060024 and RS-2024-00453036). N.T.S. was supported by São Paulo Research Foundation (FAPESP – 2017/04138-8).

Appendix A. Supplementary data

Supplementary data to this article can be found online at https://doi.org/10.1016/j.abb.2025.110331.

Abbreviations

STAT3	signaling transducer and activator of transcription 3
JAK	Janus kinase
PTP	Protein tyrosine phosphatase
SDS-PAGE	sulfate-polyacrylamide gel electrophoresis
c/w	Cells per well
FBS	Fetal bovine serum
PARP	Poly (ADP-ribose) polymerase
NT	non-treated
NAC	N-acetylcysteine;
UPR	unfolded protein response
CHX	cycloheximide

Data availability

Data will be made available on request.

References

[1] R.L. Siegel, K.D. Miller, A. Jemal, Cancer statistics, CA Cancer J. Clin. 70 (1) (2020) 7–30, 2020.
[2] M. Kirby, C. Hirst, E.D. Crawford, Characterising the castration-resistant prostate cancer population: a systematic review, Int. J. Clin. Pract. 65 (11) (2011) 1180–1192.
[3] T. Chandrasekar, J.C. Yang, A.C. Gao, C.P. Evans, Mechanisms of resistance in castration-resistant prostate cancer (CRPC), Transl. Androl. Urol. 4 (3) (2015) 365–380.
[4] T. Karantanos, P.G. Corn, T.C. Thompson, Prostate cancer progression after androgen deprivation therapy: mechanisms of castrate resistance and novel therapeutic approaches, Oncogene 32 (49) (2013) 5501–5511.
[5] M. Cai, X.L. Song, X.A. Li, M. Chen, J. Guo, D.H. Yang, Z. Chen, S.C. Zhao, Current therapy and drug resistance in metastatic castration-resistant prostate cancer, Drug Resist. Updates 68 (2023) 100962.
[6] S. Elmore, Apoptosis: a review of programmed cell death, Toxicol. Pathol. 35 (4) (2007) 495–516.

[7] D. Kashyap, V.K. Garg, N. Goel, Intrinsic and extrinsic pathways of apoptosis: role in cancer development and prognosis, Adv. Protein Chem. Struct. Biol. 125 (2021) 73–120.
[8] X. Wang, Y. Lin, Tumor necrosis factor and cancer, buddies or foes? Acta Pharmacol. Sin. 29 (11) (2008) 1275–1288.
[9] A. Ashkenazi, V.M. Dixit, Death receptors: signaling and modulation, Science 281 (5381) (1998) 1305–1308.
[10] S. Sperandio, I. de Belle, D.E. Bredesen, An alternative, nonapoptotic form of programmed cell death, Proc. Natl. Acad. Sci. U. S. A. 97 (26) (2000) 14376–14381.
[11] D. Kessel, Paraptosis and photodynamic therapy: a progress report, Photochem. Photobiol. 96 (5) (2020) 1096–1100.
[12] F. Pentimalli, S. Grelli, N. Di Daniele, G. Melino, I. Amelio, Cell death pathologies: targeting death pathways and the immune system for cancer therapy 20 (7) (2019) 539–554.
[13] D. Wendlocha, R. Kubina, K. Krzykawski, A. Mielczarek-Palacz, Selected flavonols targeting cell death pathways in cancer therapy: the latest achievements in research on apoptosis, autophagy, necroptosis, pyroptosis, ferroptosis, and cuproptosis, Nutrients 16 (8) (2024).
[14] B.A. Carneiro, W.S. El-Deiry, Targeting apoptosis in cancer therapy, Nat. Rev. Clin. Oncol. 17 (7) (2020) 395–417.
[15] M.H. Yang, I.J. Ha, S.G. Lee, J. Lee, J.Y. Um, G. Sethi, K.S. Ahn, Brassinin induces apoptosis, autophagy, and paraptosis via MAPK signaling pathway activation in chronic myelogenous leukemia cells, Biology (Basel) 12 (2) (2023).
[16] H. Yu, D. Pardoll, R. Jove, STATs in cancer inflammation and immunity: a leading role for STAT3, Nat. Rev. Cancer 9 (11) (2009) 798–809.
[17] U. Bharadwaj, M.M. Kasembeli, P. Robinson, D.J. Tweardy, Targeting Janus kinases and signal transducer and activator of transcription 3 to treat inflammation, fibrosis, and cancer: rationale, progress, and caution, Pharmacol. Rev. 72 (2) (2020) 486–526.
[18] K.S. Ahn, Special issue "role of STAT3 in oncogenesis", Biomedicines 10 (11) (2022).
[19] J. Zhang, Y.Y. Jung, C.D. Mohan, A. Deivasigamani, A. Chinnathambi, S.A. Alharbi, K.S. Rangappa, K.M. Hui, G. Sethi, K.S. Ahn, Nimbolide enhances the antitumor effect of docetaxel via abrogation of the NF-kappaB signaling pathway in prostate cancer preclinical models, Biochim. Biophys. Acta Mol. Cell Res. 1869 (12) (2022) 119344.
[20] B.B. Aggarwal, G. Sethi, K.S. Ahn, S.K. Sandur, M.K. Pandey, A.B. Kunnumakkara, B. Sung, H. Ichikawa, Targeting signal-transducer-and-activator-of-transcription-3 for prevention and therapy of cancer: modern target but ancient solution, Ann. N. Y. Acad. Sci. 1091 (2006) 151–169.
[21] D.E. Johnson, R.A. O'Keefe, J.R. Grandis, Targeting the IL-6/JAK/STAT3 signalling axis in cancer, Nat. Rev. Clin. Oncol. 15 (4) (2018) 234–248.
[22] Y.Y. Jung, N.T. Son, C.D. Mohan, J.K. Bastos, N.D. Luyen, L.M. Huong, K.S. Ahn, Kaempferide triggers apoptosis and paraptosis in pancreatic tumor cells by modulating the ROS production, SHP-1 expression, and the STAT3 pathway, IUBMB Life (2024).
[23] X. Huang, Y. Huang, Y. Yang, S. Wei, Q. Qin, Involvement of fish signal transducer and activator of transcription 3 (STAT3) in SGIV replication and virus induced paraptosis, Fish Shellfish Immunol. 41 (2) (2014) 308–316.
[24] C.D. Mohan, M.H. Yang, S. Rangappa, A. Chinnathambi, S.A. Alharbi, T. A. Alahmadi, A. Deivasigamani, K.M. Hui, G. Sethi, K.S. Rangappa, K.S. Ahn, 3-Formylchromone counteracts STAT3 signaling pathway by elevating SHP-2 expression in hepatocellular carcinoma, Biology (Basel) 11 (1) (2021).
[25] M. Kim, L.D. Morales, I.S. Jang, Y.Y. Cho, D.J. Kim, Protein tyrosine phosphatases as potential regulators of STAT3 signaling, Int. J. Mol. Sci. 19 (9) (2018).
[26] D. Xu, C.K. Qu, Protein tyrosine phosphatases in the JAK/STAT pathway, Front. Biosci. 13 (2008) 4925–4932.
[27] E.A. Bard-Chapeau, S. Li, J. Ding, S.S. Zhang, H.H. Zhu, F. Princen, D.D. Fang, T. Han, B. Bailly-Maitre, V. Poli, N.M. Varki, H. Wang, G.S. Feng, Ptpn11/Shp2 acts as a tumor suppressor in hepatocellular carcinogenesis, Cancer Cell 19 (5) (2011) 629–639.
[28] M.H. Yang, M. Lee, A. Deivasigamani, D.D. Le, C.D. Mohan, K.M. Hui, G. Sethi, K. S. Ahn, Decanoic acid exerts its anti-tumor effects via targeting c-Met signaling cascades in hepatocellular carcinoma model, Cancers (Basel) 15 (19) (2023).
[29] N.Y. Kim, S.G. Shivanne Gowda, S.G. Lee, G. Sethi, K.S. Ahn, Cannabidiol induces ERK activation and ROS production to promote autophagy and ferroptosis in glioblastoma cells, Chem. Biol. Interact. 394 (2024) 110995.
[30] M.H. Yang, I.J. Ha, J.Y. Um, K.S. Ahn, Albendazole exhibits anti-neoplastic actions against gastric cancer cells by affecting S TAT3 and STAT5 activation by pleiotropic mechanism(s), Biomedicines 9 (4) (2021).
[31] Y.Y. Jung, N.T. Son, C.D. Mohan, J.K. Bastos, N.D. Luyen, L.M. Huong, K.S. Ahn, Kaempferide triggers apoptosis and paraptosis in pancreatic tumor cells by modulating the ROS production, SHP-1 expression, and the STAT3 pathway, IUBMB Life 76 (9) (2024) 745–759.
[32] K.M. Kainat, M.I. Ansari, N. Bano, P.R. Jagdale, A. Ayanur, M. Kumar, P.K. Sharma, Rifampicin-induced ER stress and excessive cytoplasmic vacuolization instigate hepatotoxicity via alternate programmed cell death paraptosis in vitro and in vivo, Life Sci. 333 (2023) 122164.
[33] S. Zou, Q. Tong, B. Liu, W. Huang, Y. Tian, X. Fu, Targeting STAT3 in cancer immunotherapy, Mol. Cancer 19 (1) (2020) 145.
[34] W. Jin, Role of JAK/STAT3 signaling in the regulation of metastasis, the transition of cancer stem cells, and chemoresistance of cancer by epithelial-mesenchymal transition, Cells 9 (1) (2020).
[35] Y.H. Dinakar, H. Kumar, S.L. Mudavath, R. Jain, R. Ajmeer, V. Jain, Role of STAT3 in the initiation, progression, proliferation and metastasis of breast cancer and strategies to deliver JAK and STAT3 inhibitors, Life Sci. 309 (2022) 120996.
[36] Y.Y. Jung, C. Kim, M.K. Shanmugam, A. Deivasigamani, A. Chinnathambi, S. A. Alharbi, K.S. Rangappa, K.M. Hui, G. Sethi, C.D. Mohan, K.S. Ahn, Leonurine ameliorates the STAT3 pathway through the upregulation of SHP-1 to retard the growth of hepatocellular carcinoma cells, Cell. Signal. 114 (2024) 111003.
[37] D. Lee, I.Y. Kim, S. Saha, K.S. Choi, Paraptosis in the anti-cancer arsenal of natural products, Pharmacol. Ther. 162 (2016) 120–133.
[38] C.H. Dai, L.R. Zhu, Y. Wang, X.P. Tang, Y.J. Du, Y.C. Chen, J. Li, Celastrol acts synergistically with afatinib to suppress non-small cell lung cancer cell proliferation by inducing paraptosis, J. Cell. Physiol. 236 (6) (2021) 4538–4554.
[39] K. Ghosh, S. De, S. Das, S. Mukherjee, S. Sengupta Bandyopadhyay, Withaferin A induces ROS-mediated paraptosis in human breast cancer cell-lines MCF-7 and MDA-MB-231, PLoS One 11 (12) (2016) e0168488.
[40] F. Peng, M. Liao, R. Qin, S. Zhu, C. Peng, L. Fu, Y. Chen, B. Han, Regulated cell death (RCD) in cancer: key pathways and targeted therapies, Signal Transduct. Targeted Ther. 7 (1) (2022) 286.
[41] S. Sperandio, K. Poksay, I. de Belle, M.J. Lafuente, B. Liu, J. Nasir, D.E. Bredesen, Paraptosis: mediation by MAP kinases and inhibition by AIP-1/Alix, Cell Death Differ. 11 (10) (2004) 1066–1075.
[42] A.S. Lee, GRP78 induction in cancer: therapeutic and prognostic implications, Cancer Res. 67 (8) (2007) 3496–3499.
[43] C. Hetz, B. Mollereau, Disturbance of endoplasmic reticulum proteostasis in neurodegenerative diseases, Nat. Rev. Neurosci. 15 (4) (2014) 233–249.